Long-Term Administration of Eicosapentaenoic Acid Improves Post–Myocardial Infarction Cardiac Remodeling in Mice by Regulating Macrophage Polarization

Masayuki Takamura, MD, PhD;* Keisuke Kurokawa, MD;* Hiroshi Ootsuji, MD, PhD; Oto Inoue, MD; Hikari Okada, PhD; Ayano Nomura, MS; Shuichi Kaneko, MD, PhD; Soichiro Usui, MD, PhD

Background—Consumption of n-3 fatty acids reduces the incidence of cardiovascular mortality in populations that consume diets rich in fish oil. Eicosapentaenoic acid (EPA) is an n-3 fatty acid known to reduce the frequency of nonfatal coronary events; however, the frequency of mortality after myocardial infarction (MI) is not reduced. The aims of this study were to determine whether long-term administration of EPA regulated cardiac remodeling after MI and to elucidate the underlying therapeutic mechanisms of EPA.

Methods and Results—C57BL/6J mice were divided into control (phosphate–buffered saline–treated) and EPA-treated groups. After 28 days of treatment, the mice were subjected to either sham surgery or MI by left anterior descending coronary artery ligation. Mortality due to MI or heart failure was significantly lower in the EPA-treated mice than in the phosphate–buffered saline–treated mice. However, the incidence of cardiac rupture was comparable between the EPA-treated mice and the phosphate–buffered saline–treated mice after MI. Echocardiographic tests indicated that EPA treatment attenuated post-MI cardiac remodeling by preventing issues such as left ventricular systolic dysfunction and left ventricle dilatation 28 days after MI induction. Moreover, during the chronic remodeling phase, ie, 28 days after MI, flow cytometry demonstrated that EPA treatment significantly inhibited polarization toward proinflammatory M1 macrophages, but not anti-inflammatory M2 macrophages, in the infarcted heart. Furthermore, EPA treatment attenuated fibrosis in the noninfarcted remote areas during the chronic phase.

Conclusions—Long-term administration of EPA improved the prognosis of and attenuated chronic cardiac remodeling after MI by modulating the activation of proinflammatory M1 macrophages. (***J Am Heart Assoc***. 2017;6:e004560. DOI: 10.1161/JAHA.116.004560.)

Key Words: acute myocardial infarction • eicosapentaenoic acid • inflammation • macrophage • macrophage polarization • mouse • remodeling

O ver the last few decades early reperfusion strategies have dramatically improved survival rates following acute myocardial infarction (MI).[1] However, this improvement in survival has resulted in many patients who have survived an acute MI but are at a high risk of developing post-MI heart failure.[2] Development of heart failure after MI is closely associated with alterations in cardiac function and structure. This is referred to as cardiac remodeling. Cardiac remodeling is linked to the progression of heart failure and is associated with a poor prognosis in patients who survive acute MI. Prevention of the development of maladaptive post-MI cardiac remodeling is dependent on the quality of cardiac repair.[3] Interventions that balance inflammatory and reparative pathways are therefore therapeutic candidates for preventing cardiac remodeling after MI.

Eicosapentaenoic acid (EPA) and docosahexaenoic acid are n-3 fatty acids and are present primarily in oily fish. Observational studies of the Greenland Inuit population and Okinawa islanders indicated that the low risk of death from coronary artery disease in these populations was related to an abundance of n-3 fatty acids in their diets.[4,5] Several prospective epidemiological studies reported that high consumption of fish was associated with reduced mortality from

coronary artery disease.[6-9] These findings clearly indicated an inverse relationship between fish consumption and mortality from cardiovascular disease. Previous meta-analyses of supplementation with n-3 fatty acids have shown modest reductions in the rates of fatal and nonfatal cardiovascular events.[10-12] However, a recent meta-analysis that was limited to blinded, randomized, placebo-controlled trials indicated that n-3 fatty acid supplementation had no effect on cardiovascular outcomes.[13] Moreover, the results of clinical trials that evaluated the effects of n-3 fatty acids on mortality after MI are controversial. Some studies reported that treatment with n-3 fatty acids reduced cardiovascular mortality and morbidity after MI[10,14,15]; however, this effect was not observed in other studies.[16-18]

Although several clinical trials have evaluated n-3 fatty acids, little is known about the effect of EPA alone on cardiovascular mortality. The Japan EPA Lipid Intervention Study was the only large-scale prospective study conducted using EPA.[19] The study indicated that long-term use of EPA reduced the risk of major coronary events. In addition, a further subgroup analysis indicated that patients with preexisting coronary artery disease benefited more from EPA treatment than those without preexisting coronary artery disease. Several studies in animal models demonstrated the effects of EPA on the cardiovascular system.[20,21] However, whether EPA contributed to the development of cardiac remodeling after MI remains unclear.

Several epidemiological studies suggested that long-term treatment with n-3 fatty acids was beneficial after a nonfatal MI.[14,15] Furthermore, a previous study indicated an inverse dose-response relationship between fish consumption and fatal coronary heart disease.[22] Another study indicated that treatment of MI patients with high-dose n-3 fatty acids was associated with a reduction in adverse left ventricular (LV) remodeling and noninfarct myocardial fibrosis.[23]

In the present study we investigated the effects of a regular intake of an EPA-rich diet on the prognosis of MI. We hypothesize that long-term high-dose administration of EPA before and after MI improves chronic cardiac remodeling after MI and, thereby, inhibits the development of heart failure. To test this hypothesis, we evaluated cardiac remodeling after experimentally induced MI in mice that had undergone permanent coronary artery ligation.

Methods

Ethics Approval

All animal experiments were performed according to the procedures stated in the Guide for the Care and Use of Laboratory Animals of Kanazawa University (Kanazawa, Japan), which strictly conforms to the Guide for the Care

and Use of Laboratory Animals published by the US National Institutes of Health (Bethesda, Maryland). The protocols used were also approved by the Ethics Committee of Kanazawa University (Approval No. 143150).

Animals and Experimental Design

Male, 10-week-old, healthy C57BL/6J mice (Charles River Laboratories, Yokohama, Japan) were housed in the animal facility under a 12:12-hour light-dark cycle (lights on at 9 AM, lights off at 9 PM) and were fed standard mouse chow and water ad libitum. The mice were randomly divided into the following treatment groups: sham+phosphate–buffered saline (PBS) (n=18), MI+PBS (n=90), sham+EPA (n=18), and MI+EPA (n=90). EPA ethyl ester (>99% purity) was provided by Mochida Pharmaceutical Co, Ltd (Tokyo, Japan). PBS (control groups) and EPA ethyl ester (1 g/[kg·d] as a high dose of EPA) were administered to the mice by oral gavage. The mice were treated with PBS or EPA once daily for 4 weeks before and 4 weeks after experimentally induced MI.

Surgical Procedures

MI was induced by left coronary artery ligation.[24] Surgeries were performed blinded to the treatment. The mice were administered sodium pentobarbital (100 mg/kg) intraperitoneally to induce anesthesia. The animals were subsequently intubated and ventilated with air using a small-animal respirator. The chest wall was shaved and a thoracotomy was performed in the third left intercostal space. With the left ventricle in sight, the pericardial sac was excised. The left anterior descending artery was then permanently ligated with a 7-0 nylon suture at the point of its emergence from the left atrium. Significant color changes at the ischemic area were considered indicative of successful coronary occlusion. The thoracotomy was closed with 7-0 nylon sutures. The same procedure was performed for sham-operated mice except that the ligatures were left untied. The endotracheal tube was removed once spontaneous respiration resumed. The mice were placed on a heating pad maintained at 37°C until they were completely awake. The mice were reanesthetized 1, 4, 7, or 28 days after the operation, followed by euthanasia. The heart and lungs of each animal were removed immediately and weighed. The left ventricle was snap-frozen in liquid nitrogen and stored at −80°C until needed for analysis.

Survival Analysis

Survival analysis was performed in the mice that underwent surgery for MI induction. During the 28-day study period after MI induction, the cages were inspected daily for dead mice. All dead mice were examined for the presence of MI and

either pulmonary congestion or blood clots around the heart and in the thoracic cavity. The cause of death was classified as either congestive heart failure or cardiac rupture. On autopsy, large blood clots around the heart and within the thoracic cavity, in combination with perforation of the infarcted wall, indicated cardiac rupture and pulmonary congestion with fluid accumulation in the chest indicated heart failure. In the survival analysis we did not include the mice that were sacrificed at intermediate time points.

Echocardiography

An echocardiographic study was performed under anesthesia with tracheal intubation under a respirator before euthanasia 1, 4, 7, and 28 days after MI. The mice were anesthetized by isoflurane inhalation. Echocardiographic data were obtained by an ultrasonographer experienced in rodent imaging using a 12-MHz transducer (SONOS 5500; Agilent Technologies, Santa Clara, CA). The ultrasonographer was blinded to the treatment groups. Short-axis, 2-dimensional echocardiographic images were acquired at papillary levels. Three consecutive cardiac cycles were used for each measurement. LV end-diastolic diameter (LVEDD) and end-systolic diameter (LVESD) were measured at end-diastole and end-systole, respectively. Percentage fractional shortening (%FS) and LV ejection fraction (LVEF) were calculated using the following formulas:

$$\%FS = [(LVEDD - LVESD)/LVEDD] \times 100$$

$$LVEF\,(\%) = 100 \times (LVEDD^3 - LVESD^3)/LVEDD^3$$

Cell Isolation and Flow Cytometric Analysis

To obtain single-cell suspensions, the hearts of the mice were initially perfused with PBS. The hearts were then pooled in a cell culture dish, washed thoroughly with Hanks' Balanced Salt Solution, and minced using a sterile surgical blade. The cardiac tissues were enzymatically digested with the aid of a mouse Tumor Dissociation Kit (Miltenyi Biotec, Bergisch Gladbach, Germany). GentleMACS Dissociators (Miltenyi Biotech) were used in the mechanical dissociation steps. After dissociation, the samples were filtered to remove any remaining large particles from the single-cell suspensions. $CD45^+$ cells were then isolated using the MACS Microbeads Technology (Miltenyi Biotec). $CD45^+$ cells were positively selected using CD45 Microbeads (Miltenyi Biotec). Cell suspensions were stained with FITC Rat Anti-Mouse CD11b (BD Biosciences, San Jose, CA), PE Hamster Anti-Mouse CD11c (BD Biosciences), PerCP/Cy5.5 Anti-Mouse F4/80 (BioLegend, San Diego, CA), and Alexa Fluor 647 Anti-Mouse CD206 (MMR) (BioLegend).

Within the myeloid-lineage leukocyte population, macrophages were defined to be $CD45^+CD11b^+F4/80^+$. Sorted $CD45^+CD11b^+F4/80^+$ macrophages derived from the myocardium were further divided into $CD11c^+CD206^-$ M1 and $CD11c^-CD206^+$ M2 macrophage populations. Fluorescence compensation controls and fluorescence-minus-1 stain sets were used to accurately identify cells within multicolor-stained samples. Cells were analyzed using a BD Accuri C6 cytometer (BD Biosciences). The data were analyzed using FlowJo software (Tree Star, Inc, Ashland, OR).

Collagen Morphometric and Fibrosis Analysis

Morphometric analysis of collagen and fibrosis was performed using 6-μm paraffin short-axis sections at the apical, mid, and basal LV levels stained with picro-sirius red and AZAN, respectively. Quantitative assessments of collagen accumulation and fibrotic area were performed on at least 20 randomly chosen high-power fields in each section of the noninfarcted area. Collagen volume fraction and fibrosis were calculated as the ratio of the total area of collagen and fibrosis to the myocyte area in the entire visual field of the section, using Image J software (National Institutes of Health, Bethesda, MD). The perivascular and pericardial areas were excluded from the measurements. All manual counts were performed in a blinded fashion.

LV Myocyte Cross-Sectional Area

Myocyte cross-setional area was measured from images captured from hematoxylin-eosin–stained sections as previously described.[25] Suitable cross sections were defined as having nearly circular capillary profiles and circular-to-oval myocyte sections. The outlines of 100 myocytes were traced in each section of the noninfarcted area, using Image J software. All manual counts were performed in a blinded fashion.

Immunohistochemical Analysis

Paraffin-embedded heart tissue sections were stained with anti-F4/80 antibodies (1:200 dilution; AbD Serotec, Cedar-Lane Labs, Burlington, ON, Canada) to identify the F4/80 antigen expressed by macrophages. Alexa Fluor 488 Donkey Anti-Rat IgG (Invitrogen, Carlsbad, CA) was used as a secondary antibody to detect $F4/80^+$ cells. The total number of nuclei and the number of nuclei in F4/80-expressing cells were counted in each field. The fraction of F4/80-expressing cells in each sample was calculated as the sum of the number of nuclei in F4/80-expressing cells divided by the total number of nuclei in different sections of a sample. Quantitative assessments of the number of nuclei were performed

on at least 20 randomly chosen high-power fields in each section of the noninfarcted area. All manual counts were performed in a blinded fashion.

Quantitative Real-Time Detection Polymerase Chain Reaction

Total RNA was prepared from mouse hearts using the RNeasy Fibrous Tissue Mini Kit (QIAGEN, Chatsworth, CA). Real-time polymerase chain reaction (PCR) analysis was carried out using TaqMan gene expression assays and the Universal PCR master mix (Applied Biosystems, Foster City, CA), using an ABI prism 7900 Sequence Detection System (Applied Biosystems). The primers used included mouse atrial natriuretic peptide (ANP) (Mm01255748_g1), B-type natriuretic peptide (BNP) (Mm01255770_g1), collagen type I α 1 (Mm00801666_g1), collagen type III α 1 (Mm01254476_m1), interleukin-6 (IL-6) (Mm01210733_m1), transforming growth factor-β1 (TGF-β1) (Mm00441726_m1), EGF-like module-containing mucin-like hormone receptor-like 1 (EMR1) (Mm00802530_m1), mannose receptor C type 1 (MRC1) (Mm00485148_m1), chemokine (C-C motif) ligand 2 (CCL2) (Mm00441242_m1), vascular endothelial growth factor (VEGF) A (Mm 00437306_m1), interferon regulatory factor 5 (IRF5) (Mm00496477_m1), and glyceraldehyde 3-phosphate dehydrogenase (GAPDH) (Mm99999915_g1). Relative mRNA transcript levels (5-8 biological replicates with 3 technical replicates each) were quantified using the $2^{-\Delta\Delta CT}$ method; *GAPDH* was used as an internal control.

Western Blotting

Whole-cell lysates from mouse hearts were washed in PBS and lysed using CelLytic MT Cell Lysis Reagent (Sigma-Aldrich, St. Louis, MO) containing Complete Protease Inhibitor Cocktail and PhosSTOP (Roche Applied Science, Indianapolis, IN). The membranes were blocked with skim milk (WAKO, Osaka, Japan) or Block Ace Powder (DS Pharma, Osaka, Japan). The following primary antibodies were used: Smad2 (1:1000 dilution), Phospho-Smad2 (Ser465/467) (1:1000 dilution), Smad3 (1:1000 dilution), Phospho-Smad3 (Ser423/425) (1:1000 dilution), IRF5 (1:1000 dilution; all Cell Signaling Technology, Danvers, MA), and GAPDH (1:1000 dilution; Santa Cruz Biotechnology, Inc, Santa Cruz, CA). Band density was analyzed using Image J software. The densitometric values (4-8 biological replicates with 3 or more technical replicates each) were normalized using a GAPDH signal.

Data Analysis

Data are presented as mean±standard error of the mean (SEM). Values were compared between the MI+PBS and MI+EPA groups using the nonparametric Mann-Whitney U test. Survival was compared using the log-rank test. $P \leq 0.05$ was considered statistically significant. Survival curves were analyzed using Kaplan-Meier log-rank (Mantel-Cox) tests. Stated n values are biological replicates. Statistical analyses were performed using GraphPad Prism 6.03 (GraphPad Software, Inc, San Diego, CA).

Results

Mortality After MI Was Reduced in EPA-Treated Mice

To explore the effects of EPA after MI, we monitored mice that were administered EPA or PBS for 4 weeks after sham and MI operations. All mice in the sham+PBS and sham+EPA groups survived over the course of the 28-day study (Figure 1A). The incidence of postinfarct mortality was significantly lower in the MI+EPA group than in the MI+PBS group (59.3% vs 41.2%, $P=0.0361$). We also found that the incidence of death due to heart failure after MI was significantly higher in the MI+PBS group than in the MI+EPA group (20.6% vs 6.8%, $P=0.0102$; Figure 1B). However, the occurrence of cardiac rupture was similar between the MI+PBS and MI+EPA groups (38.2% vs 33.9%, $P=0.4248$; Figure 1C). The results indicated that EPA treatment prevented death from heart failure following coronary artery ligation. The results further indicated that EPA played an important role in cardiac remodeling after MI and was beneficial for preventing postinfarct heart failure.

Heart Failure and Cardiac Dysfunction Were Attenuated in EPA-Treated Mice

The ratios of heart weight to tibial length and lung weight to tibial length, which are indicative of cardiac hypertrophy and lung edema, were similar between the sham+PBS and sham+EPA groups 28 days after the sham operation. Twenty-eight days after coronary artery ligation, EPA administration significantly decreased both ratios (Figure 2A and 2B).

The mRNA expression levels of *ANP* and *BNP* in the left ventricle were similar between the sham+PBS and sham+EPA groups 28 days after the sham operation but were significantly lower in the MI+EPA group than in the MI+PBS group 28 days after MI (Figure 2C and 2D). Given that *ANP* and *BNP* are markers of heart failure, these results indicated that the EPA treatment improved heart failure after MI.

Echocardiographic tests indicated that LVEF, %FS, LVEDD, and LVESD were comparable between the sham+PBS and sham+EPA groups 28 days after the sham operation. A greater deterioration in LV systolic function was observed in the MI+PBS group than in the MI+EPA group 28 days after MI.
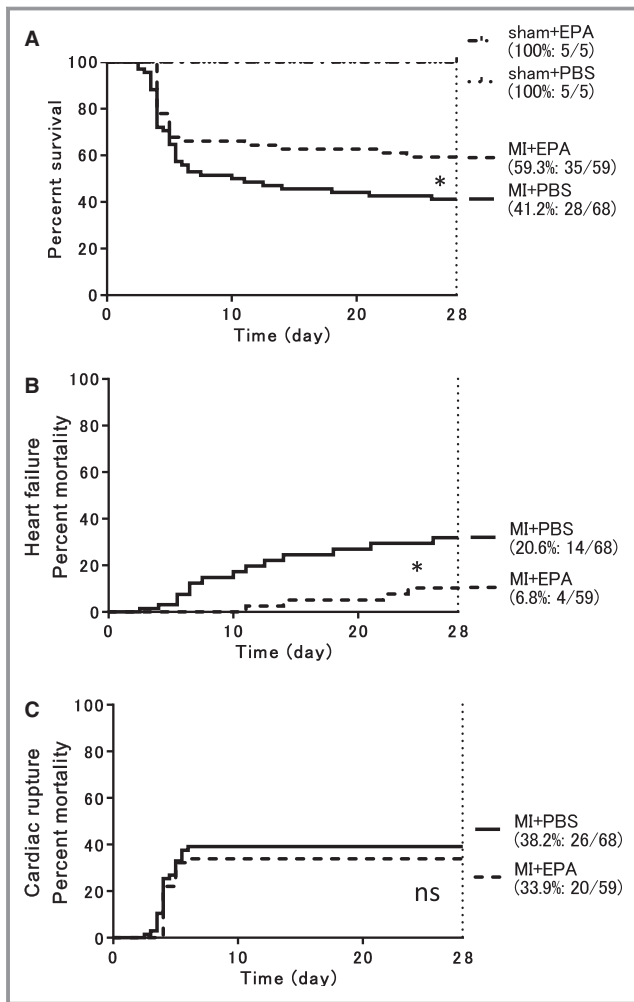
Figure 1. EPA improved mortality from heart failure after MI, but it did not improve mortality from cardiac rupture. A, Kaplan-Meier survival plot representing the percentage of surviving mice subjected to sham surgery with PBS treatment (sham+PBS, n=5), sham surgery with EPA treatment (sham+EPA, n=5), coronary ligation with PBS treatment (MI+PBS, n=68), or coronary ligation with EPA treatment (MI+EPA, n=59). Mortality from congestive heart failure (B) and cardiac rupture (C) after MI induction in mice by coronary artery ligation. In the survival analysis we did not include the mice that were sacrificed at intermediate time points. Differences between groups were tested by the log-rank test. *P<0.05, comparing the MI+PBS and MI+EPA groups. EPA indicates eicosapentaenoic acid; MI, myocardial infarction; PBS, phosphate-buffered saline.

LVEF and %FS were used to evaluate LV systolic function. LVEDD and LVESD were significantly larger in the MI+PBS group than in the MI+EPA group 28 days after MI (Figure 2E). Data from the survival analysis revealed that the good clinical outcomes in the MI+EPA group were associated with an alleviation of death owing to heart failure after MI (Figure 1). The mRNA expression levels of *ANP* and *BNP* and the weights of the hearts and lungs of the mice indicated

that the EPA treatment had therapeutic effects on post-MI heart failure within 7 days after MI (Figure S1). However, LVEF, %FS, LVEDD, and LVESD were comparable between the MI+PBS and MI+EPA groups within 7 days after MI (Figure S2). Echocardiographic tests revealed that EPA treatment had a high impact on structural cardiac remodeling 28 days after MI. To understand the therapeutic effects of EPA on cardiac remodeling, which contributes to the development of heart failure after MI, we analyzed the mechanisms underlying the aforementioned phenomena 28 days after MI. The 28-day period after MI is referred to as the remodeling phase.[26]

EPA Treatment Inhibited Polarization Toward Proinflammatory M1 Macrophages During the Remodeling Phase

Macrophages play a central role in wound healing and tissue regeneration, such as occurs after ischemic injury. The functions of and balance between the activities of proinflammatory M1 and anti-inflammatory M2 macrophages determine the direction of remodeling.[27]

We focused on the macrophage population in the heart 28 days after MI and applied a rigorous flow cytometry gating strategy to exclude measuring potential infiltrating leukocytes (Figure 3A). To determine the total CD45$^+$ cell and macrophage numbers that were recruited into the infarcted hearts, we analyzed all the cells that were isolated from whole left ventricles using CD45 microbeads. Macrophages were defined as cells with a dual expression of CD11b (Mac-1) and F4/80 surface markers.[28] Flow cytometry results indicated that there were no significant differences in the total number of CD45$^+$ cells and macrophages infiltrated into the left ventricle between the MI+PBS and MI+EPA groups 28 days after MI. (Figure 3B through 3D). CD11c and CD206 expression were used to subclassify the macrophages as either M1 (proinflammatory, CD11c$^+$CD206$^-$) or M2 (anti-inflammatory, CD11c$^-$CD206$^+$) by flow cytometry.[29–31] Although not entirely specific (ie, inclusion of dendritic cells), CD11c is a frequently used cell surface marker for proinflammatory M1 macrophages and monocytes. Additionally, the post-MI frequency of cardiac dendritic cells is much lower (fewer than 1 in 20 cells) than that of cardiac macrophages.[32] This suggested that contamination of the CD11c$^+$ cardiac cells by dendritic cells was insignificant. Therefore, in our study, we used CD11c as an M1 marker. As shown in Figure 3E, M2 macrophages were more abundant than M1 macrophages in the hearts of the mice. These data were consistent with those from a previous study.[33] We observed that in the 2 mouse groups with MI, the percentage of M1 macrophages was significantly higher in the MI+PBS group than in the MI+EPA group (Figure 3F; 7.6±0.4% vs 5.4±0.6%,
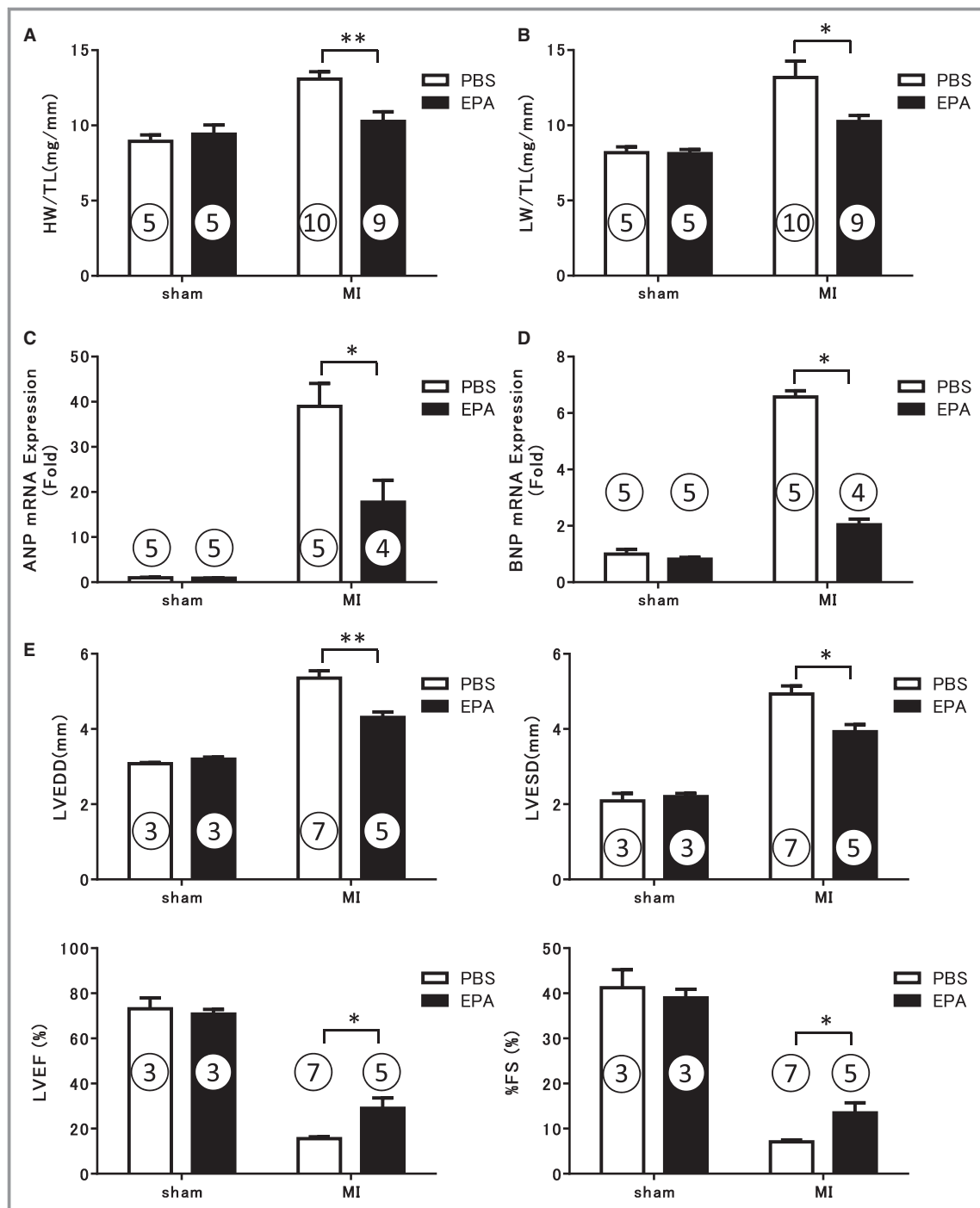
Figure 2. EPA attenuated cardiac remodeling and congestive heart failure after MI. Ratio of (A) heart weight to tibial length (HW/TL) and (B) lung weight to tibial length (LW/TL), calculated 28 days after the MI and sham operations (n=5-10 biological replicates per group). Cardiac mRNA expression levels of (C) *ANP* and (D) *BNP* 28 days after coronary artery ligation and the sham operations were determined by RTD-PCR (n=4-5 biological replicates per group). E, Echocardiographic analyses of the EPA- and PBS-treated groups 28 days after coronary artery ligation and the sham operations. Data are presented as mean±standard error of the mean (n=3-7 biological replicates per group). Values were compared between the MI+PBS and MI+EPA groups using the nonparametric Mann-Whitney U test. *$P<0.05$, **$P<0.01$, comparing the MI+PBS and MI+EPA groups. %FS indicates percentage fractional shortening; ANP, atrial natriuretic peptide; BNP, B-type natriuretic peptide; EPA, eicosapentaenoic acid; LVEDD, left ventricular end-diastolic diameter; LVEF, left ventricular ejection fraction; LVESD, left ventricular end-systolic diameter; MI, myocardial infarction; PBS, phosphate-buffered saline; RTD-PCR, real-time detection polymerase chain reaction.
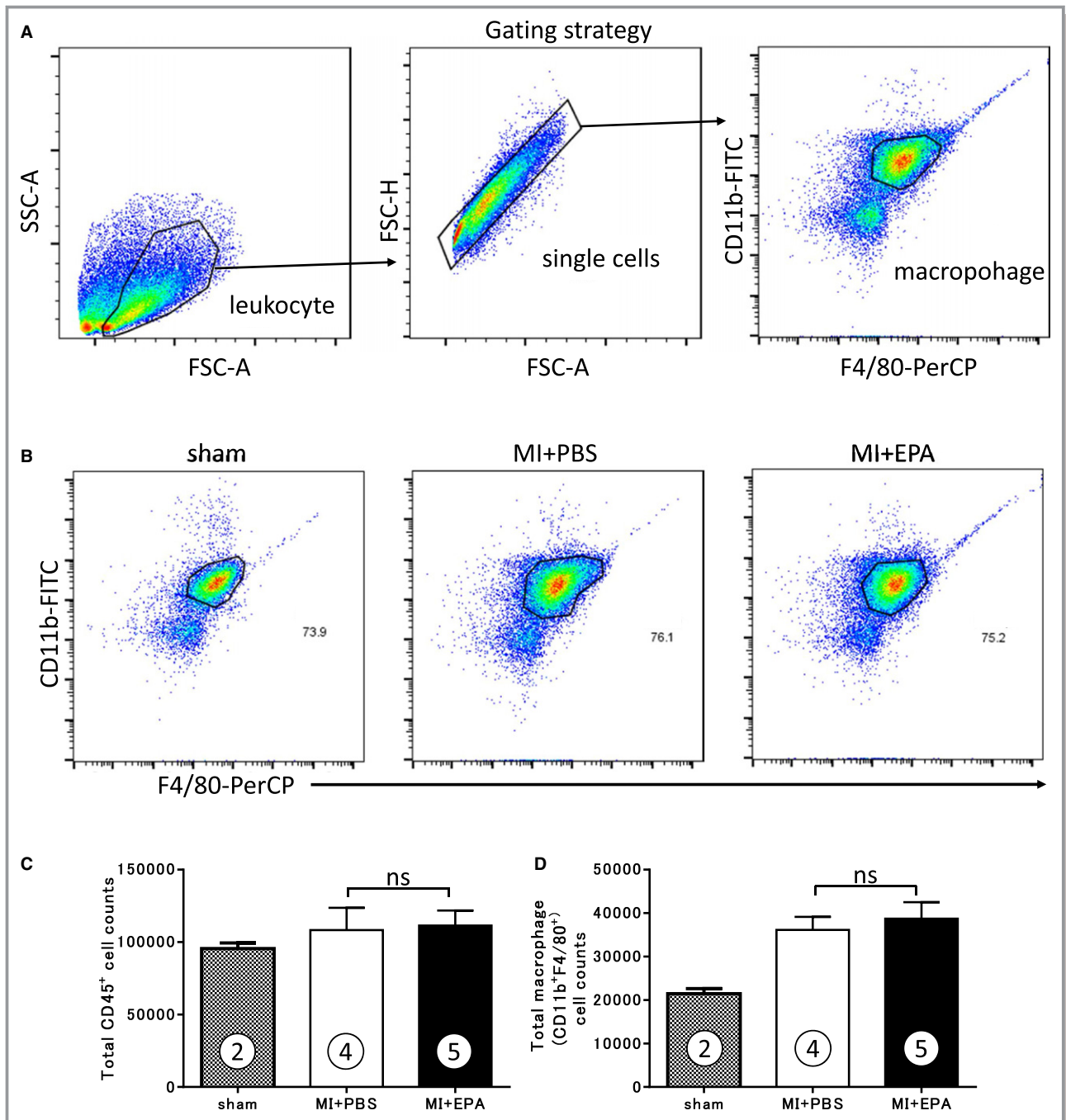
Figure 3. EPA treatment inhibited polarization toward proinflammatory M1-like macrophages in myocardial tissue after MI. A, Gating strategy after purification of $CD45^+$ cells by MACS separation of leukocytes (identified as SSC^{low} and FSC^{high}), single cells (doublet discrimination), and heart macrophages (identified as $CD11b^+F4/80^+$). B and E, Representative images of flow cytometric analysis of the sham, MI+PBS, and MI+EPA treatment groups 28 days after surgery. B, Scatter plots identifying cardiac-residing $CD11b^+F4/80^+$ macrophages. E, Scatter plots identifying cardiac-residing M1 macrophages (proinflammatory; $CD11c^+CD206^-$) and M2 macrophages (anti-inflammatory; $CD11c^-CD206^+$). Flow cytometric quantification of (C) total $CD45^+$ cell counts, (D) total macrophage $(CD11b^+F4/80^+)$ cell counts, (F) the percentage of M1 macrophage (proinflammatory, $CD11c^+$ $CD206^-$), (G) the ratio of M1 (proinflammatory, $CD11c^+$ $CD206^-$) to M2 (anti-inflammatory, $CD11c^-CD206^+$) macrophages, (H) the percentage of total macrophage $(CD11b^+F4/80^+)$, and (I) the percentage of M2 macrophage (anti-inflammatory, $CD11c^-CD206^+$) in the hearts of the sham, MI+PBS, and MI+EPA groups 28 days after the MI and sham operations. Data are presented as mean±standard error of the mean (n=2-5 biological replicates per group). Values were compared between the MI+PBS and MI+EPA groups using the nonparametric Mann-Whitney U test. *$P<0.05$, comparing the MI+PBS and MI+EPA groups. EPA indicates eicosapentaenoic acid; FSC, forward scatter; MI, myocardial infarction; PBS, phosphate-buffered saline; SSC, side scatter.
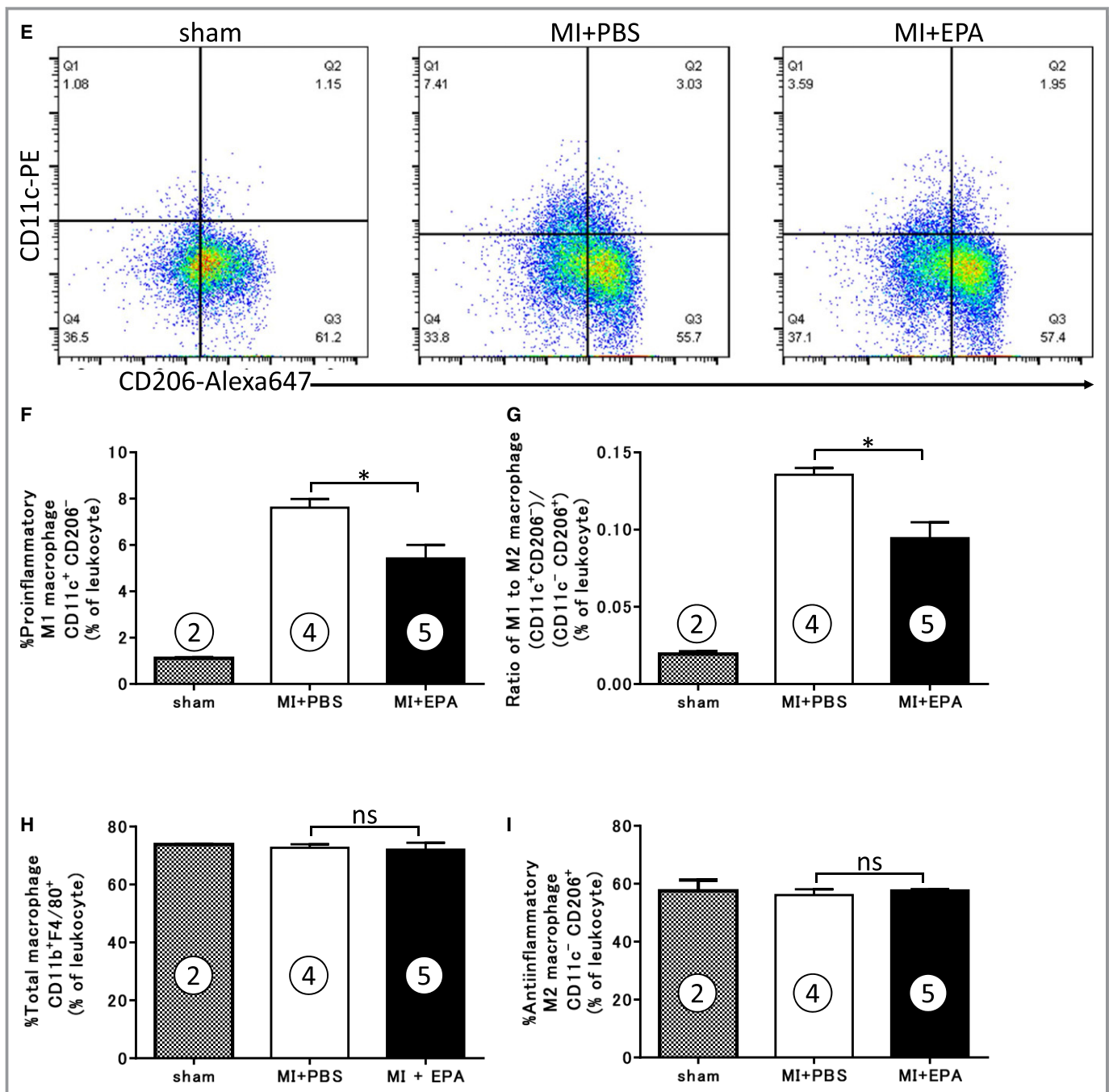
Figure 3. Continued.

P=0.0317). In addition, the ratio of M1 to M2 macrophages was significantly higher in the MI+PBS group than in the MI+EPA group (Figure 3G; 0.1355±0.004% vs 0.0944± 0.010%, *P*=0.0317). However, the percentage of CD11b⁺F4/ 80⁺ macrophages in the MI+PBS group was similar to that in the MI+EPA group (Figure 3H; 72.73±1.2% vs 72.0±2.4%, respectively; *P*>0.9999). The same observation was made regarding the percentage of M2 macrophages (Figure 3I; 56.1±2.0% vs 57.7±0.5%, respectively; *P*>0.9999).

Collectively, treatment with EPA inhibited polarization toward M1 macrophages in the infarcted heart, whereas the total macrophage population during the post-MI chronic phase was not affected by EPA treatment. These results indicated that the decreased population of M1 macrophages following treatment with EPA during the post-MI chronic phase was attributable to attenuated polarization toward M1 macrophages but not attenuated macrophage recruitment from outside of the heart. Therefore, EPA

treatment may render the chronic infarcted heart milieu anti-inflammatory.

Gene Expression Analysis of Infarcted Hearts During the Remodeling Phase

As mentioned above, flow cytometric analysis revealed that EPA treatment attenuated inflammation in the infarcted hearts by inhibiting polarization toward proinflammatory M1 macrophages during the remodeling phase. A growing body of evidence suggests that accentuation, prolongation, or expansion of the postinfarction inflammatory response and the following fibrosis result in cardiac maladaptive remodeling and dysfunction after MI.[3] To determine whether EPA treatment had therapeutic effects on post-MI chronic remodeling, the expression level of genes associated with fibrosis and inflammation 28 days after MI was analyzed by real-time detection PCR.

It was previously reported that, during the later remodeling phase, the activation of TGF-β1 caused excessive LV interstitial fibrosis, which led to deleterious cardiac failure after MI.[34] The expression levels of the TGF-β1 gene and downstream genes, such as collagen I and collagen III, during the remodeling phase were significantly lower in the MI+EPA group than in the MI+PBS group (Figure 4A through 4C). Moreover, gene expression levels of CCL2, mucin-like hormone receptor-like 1, and IL-6, which are proinflammatory genes and are also known as M1 macrophage genes, were lower in the MI+EPA group than in the MI+PBS group. Conversely, gene expression levels of MRC1 and VEGF, which are anti-inflammatory (M2 macrophage) genes, were higher in the MI+EPA group than in the MI+PBS group (Figure 4D through 4H).

The above results indicated that EPA treatment attenuated fibrosis and inflammation in the infarcted heart during the chronic remodeling phase at the transcriptional level.

Fibrosis, Hypertrophy, and Macrophage Recruitment to Noninfarcted Areas Were Attenuated in the EPA-Treated Mice During the Post-MI Chronic Phase

The molecular and cellular changes that occur during cardiac remodeling affect both the necrotic areas and the noninfarcted areas of the ventricle. This manifests clinically as increased chamber dilatation and sphericity, myocardial hypertrophy, and worsened cardiac function.[3] The post-MI cardiac remodeling process is caused by several mechanisms, including increased interstitial fibrosis, cardiomyocyte hypertrophy, and recruitment of inflammatory cells in the remote noninfarcted area during the chronic phase.[35]

Twenty-eight days after MI, the collagen volume fraction detected by picro-sirius red staining in the noninfarcted area was significantly higher in the MI+PBS group than in the MI+EPA group (Figure 5A and 5B). Similarly, fibrosis detected by AZAN staining in the noninfarcted area 28 days after MI was significantly attenuated by EPA treatment (Figure 5C and 5D). Cross-sectional area analysis in the noninfarcted area revealed that cardiac myocyte hypertrophy was significantly inhibited by EPA treatment 28 days after MI (Figure 5E and 5F). Macrophages were defined as cells with F4/80 surface markers. F4/80 immunostaining confirmed the presence of significantly more macrophages in the noninfarcted areas of the hearts of the MI+PBS group than in those of the MI+EPA group 28 days after MI (Figure 5G and 5H).

Upregulated IRF5 During the Post-MI Chronic Phase Was Attenuated by EPA Treatment

As mentioned above, treatment with EPA inhibited polarization toward M1 macrophages in the infarcted heart during the chronic phase. We focused on IRF5 expression because IRF5 was previously reported to play a critical role in regulating macrophage polarization toward the proinflammatory M1 phenotype.[36,37] To determine the mechanism by which treatment with EPA inhibited the polarization of M1 macrophages in the infarcted heart, we analyzed the mRNA expression and protein level of IRF5 in the heart during the post-MI chronic phase.

Compared to that in sham mice, both the mRNA expression and IRF5 protein level in the post-MI heart were upregulated. EPA treatment significantly attenuated this upregulation in the infarcted heart 28 days after MI (Figure 6A and 6B).

These results indicated that macrophage polarization toward a proinflammatory milieu after MI was attenuated by EPA treatment, which regulated IRF5 transcription and translation.

TGF-β/Smad Signaling Was Attenuated in the EPA-Treated Mice During the Post-MI Chronic Phase

TGF-β/Smad signaling plays a prominent role in the context of fibrosis induction after MI. Accelerated TGF-β/Smad signaling enables phosphorylation and activation of the Smad family. Although several Smad pathways have been reported, the canonical Smad pathway, including Smad2 and Smad3, is regarded as the primary pathway of TGF-β signaling.[38] As mentioned above, the mRNA expression levels of the TGF-β1 gene and downstream fibrosis-related genes during the remodeling phase were significantly lower in the MI+EPA
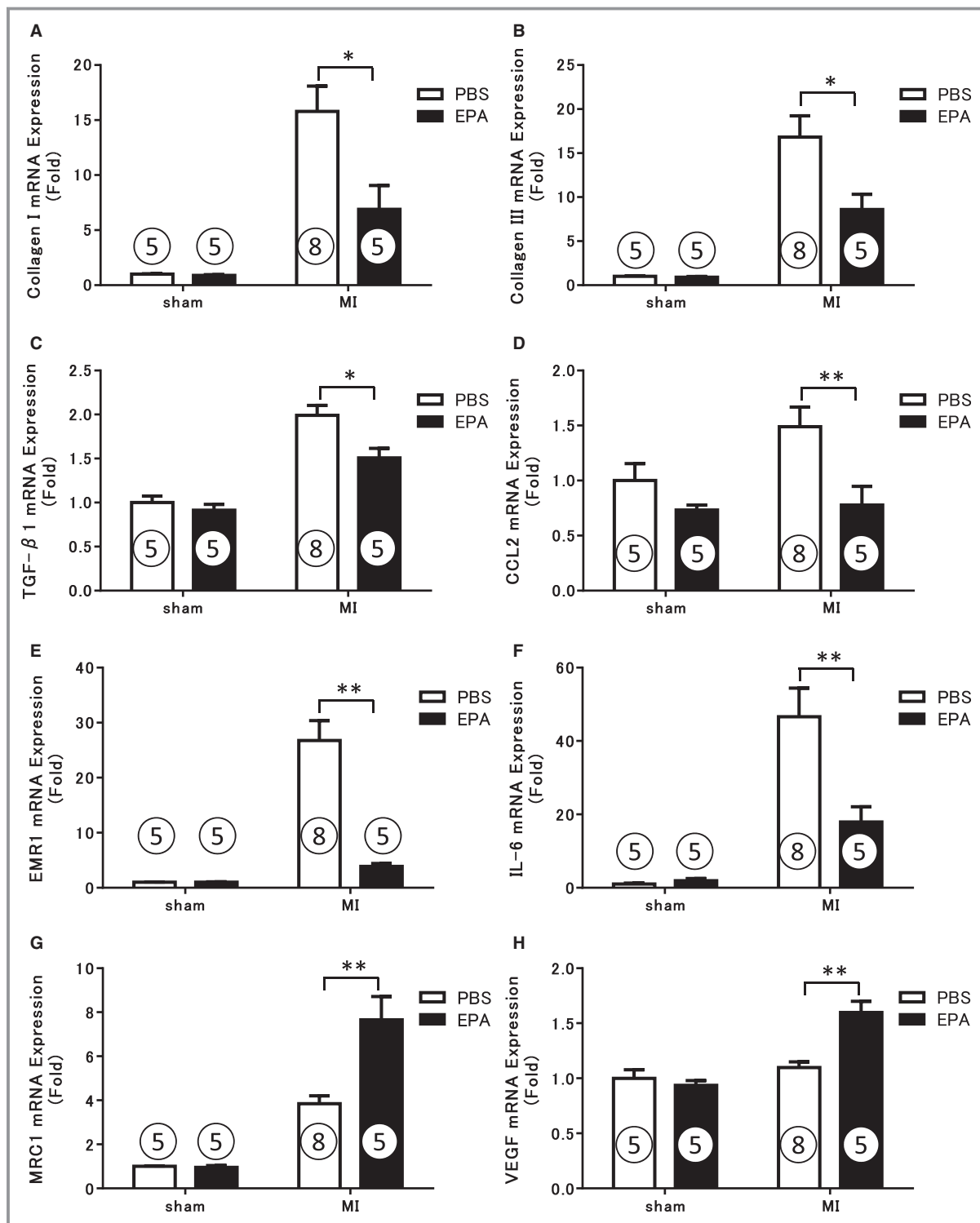
Figure 4. EPA modulated gene expression profiles in the heart 28 days after MI. The cardiac mRNA expression level of (A) *collagen I*, (B) *collagen III*, (C) *TGF-β1*, (D) *CCL2*, (E) *EMR1*, (F) *IL-6*, (G) *MRC1*, and (H) *VEGF* 28 days after coronary artery ligation and the sham operations was determined by RTD-PCR. Data are presented as mean±standard error of the mean, n=5 to 8 biological replicates per group. Values were compared between the MI+PBS and MI+EPA groups using the nonparametric Mann-Whitney U test. $*P<0.05$, $**P<0.01$, comparing the MI+PBS and MI+EPA groups. CCL2 indicates chemokine (C-C motif) ligand 2; EMR1, EGF-like module-containing mucin-like hormone receptor-like 1; EPA, eicosapentaenoic acid; IL-6, interleukin-6; MI, myocardial infarction; MRC1, mannose receptor C type 1; PBS, phosphate-buffered saline; TGF-β1, transforming growth factor-β1; VEGF, vascular endothelial growth factor.
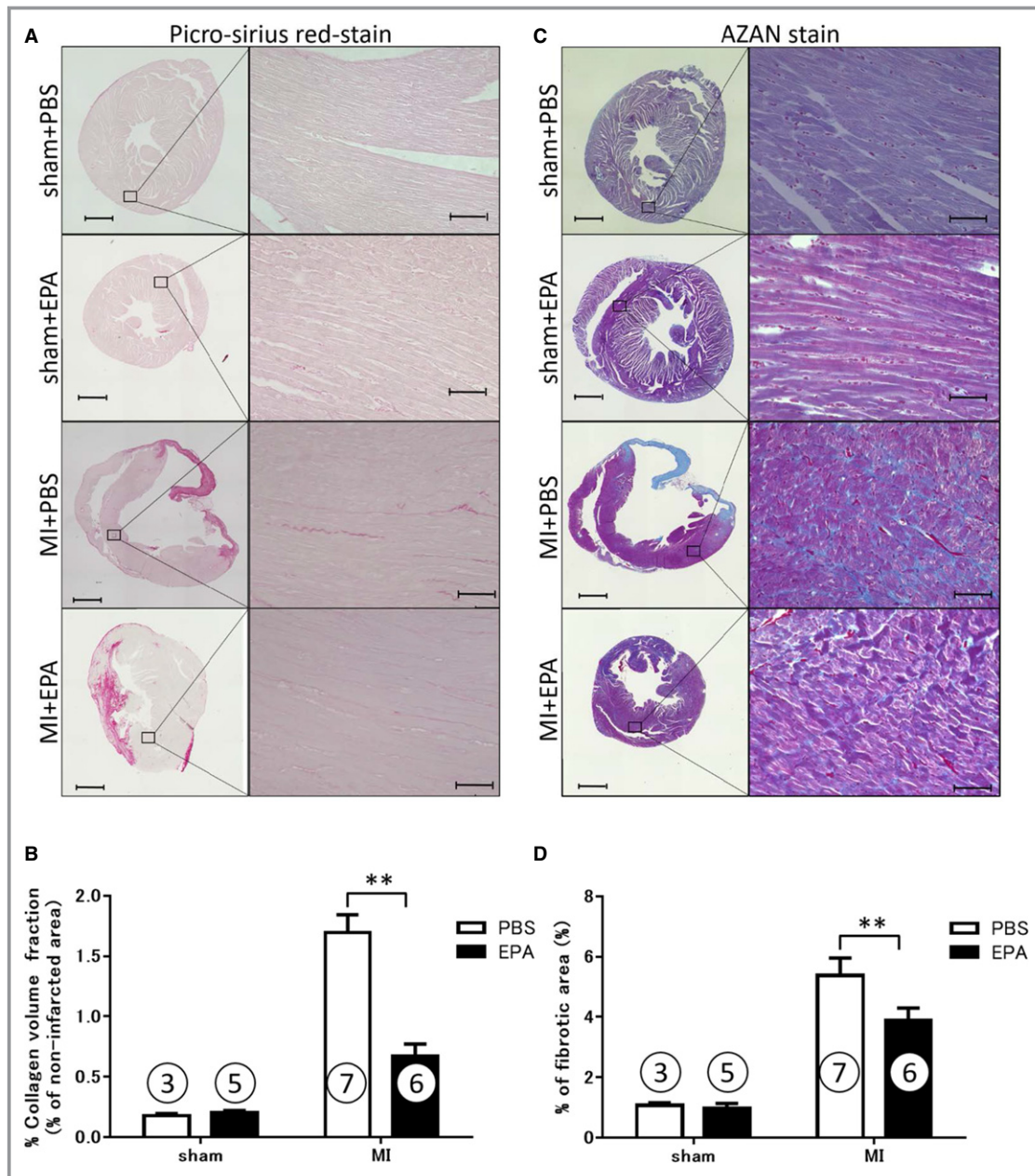
Figure 5. EPA modulated cardiac remodeling in the noninfarcted area of the mouse heart 28 days after MI. A, Overview and representative high-power photographs of picro-sirius red-stained remote LV myocardium 28 days after the MI and sham operations at mid-LV levels. Red stains indicate collagen accumulation. B, The collagen volume fractional percentage of picro-sirius red-stained remote LV myocardium. n=3 to 7 biological replicates per group. C, Overview and representative high-power photographs of AZAN-stained remote LV myocardium 28 days after the MI and sham operations at mid-LV levels. Blue stains indicate fibrosis. D, The fibrosis area percentage of AZAN-stained remote LV myocardium. n=3 to 7 biological replicates per group. E, Overview and representative high-power photographs of hematoxylin-eosin–stained remote LV myocardium 28 days after the MI and sham operations at mid-LV levels. F, Cardiac myocyte cross-sectional area in the noninfarcted myocardium was obtained at 28 days. n=5 to 9 biological replicates per group. G, Overview and representative immunohistochemical staining of F4/80 in the noninfarcted area of the mouse heart 28 days after the MI and sham operations at mid-LV levels. Immunohisto-chemical staining with F4/80 identified macrophages. Brown color indicated F4/80; blue color indicated nuclei. H, Percentage of the total number of cells that represent F4/80-positive cells in the noninfarcted myocardium. n=3 to 11 biological replicates per group. Scale bar=1000 μm (overview) and 50 μm (high power). Data are presented as mean±standard error of the mean. Values were compared between the MI+PBS and MI+EPA groups using the nonparametric Mann-Whitney U test. *$P<0.05$, **$P<0.01$, ***$P<0.001$, comparing the MI+PBS and MI+EPA groups. EPA indicates eicosapentaenoic acid; LV, left ventricle; MI, myocardial infarction; PBS, phosphate-buffered saline.
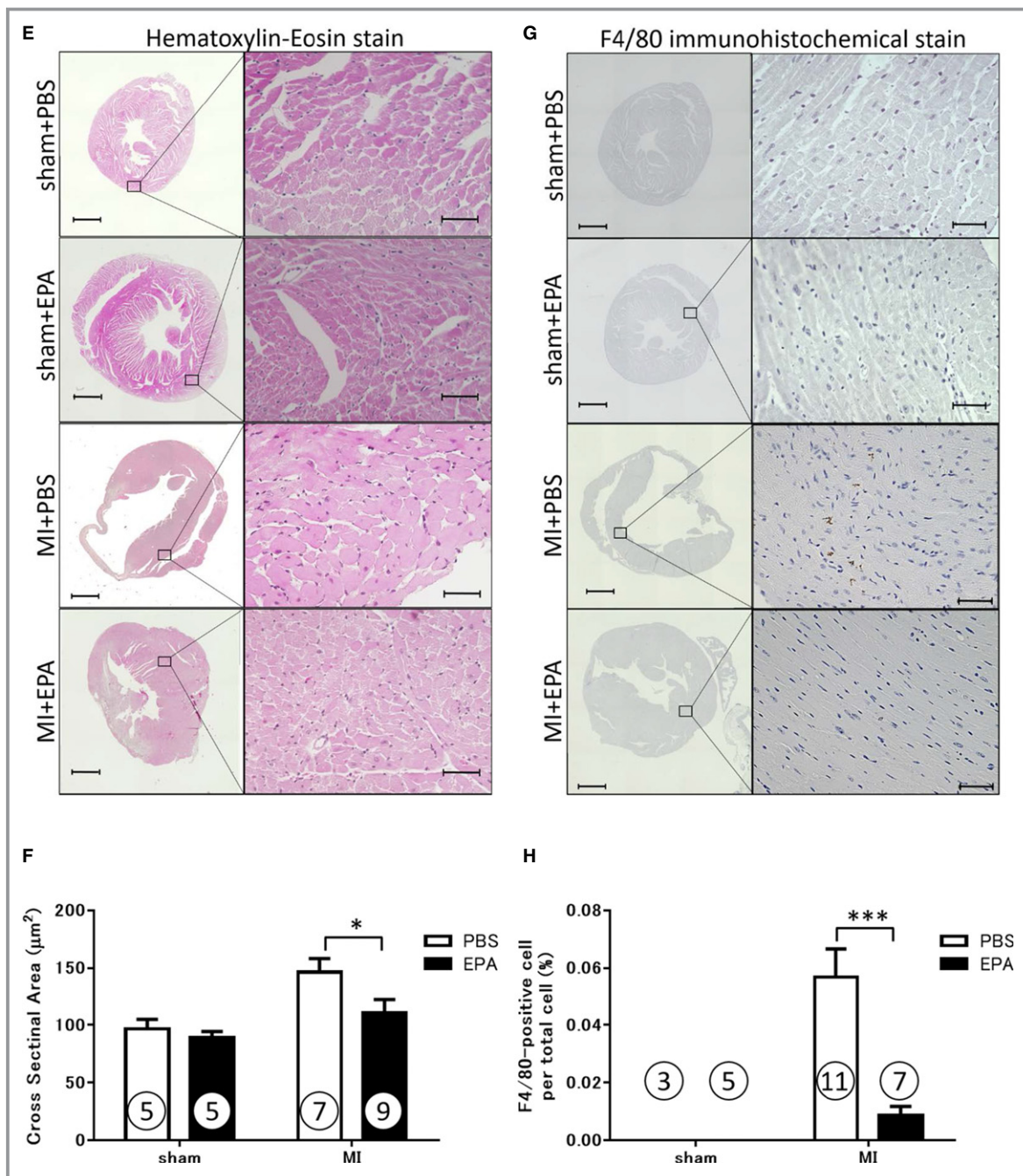
Figure 5. Continued.

group than in the MI+PBS group (Figure 4A through 4C). To determine whether EPA treatment had an impact on TGF-β activity in vivo during the post-MI chronic phase, levels of Smad2 and Smad3, as transcription factors of the canonical Smad pathway, were determined by Western blotting.

Immunoblot analysis revealed that EPA treatment significantly attenuated the phosphorylation of Smad2 and Smad3 28 days after MI (Figure 7A and 7B).

These results indicated that EPA treatment attenuated TGF-β/Smad signaling, which suggested that fibrosis was

inhibited during the chronic remodeling phase after MI by EPA treatment via TGF-β/Smad signaling.

Discussion

Several major findings were obtained in this study. First, long-term administration of high-dose EPA before and after MI reduced mortality after MI. Second, we observed that the therapeutic effect of EPA in our study was primarily due to a decrease in death from heart failure after MI. Heart failure and
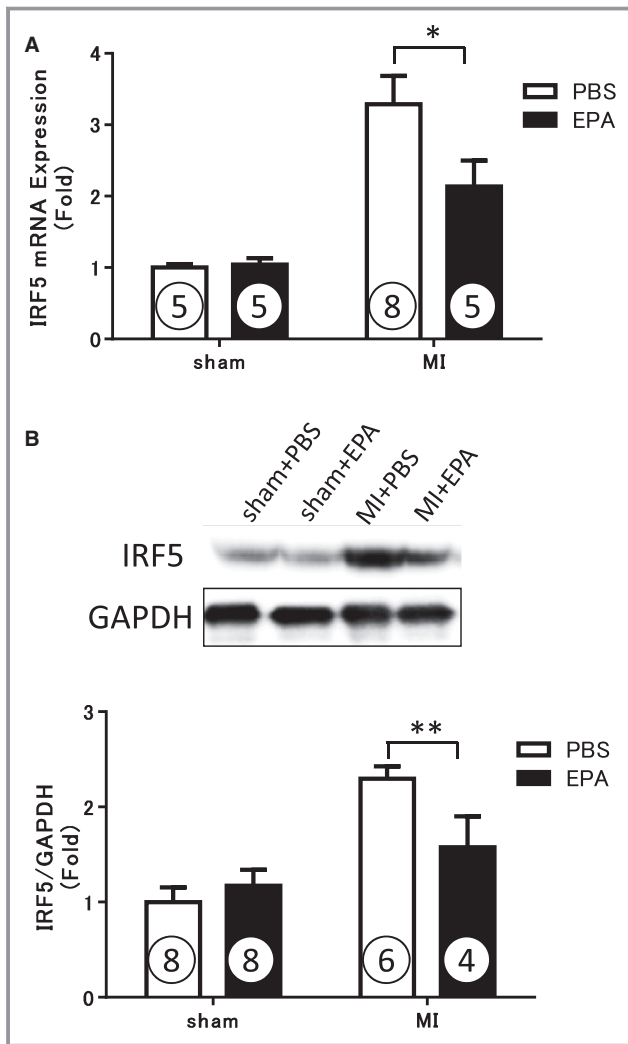
Figure 6. Upregulation of *IRF5* expression 28 days after MI was significantly attenuated by EPA treatment. A, Cardiac mRNA expression level of *IRF5* 28 days after coronary artery ligation and the sham operations was determined by RTD-PCR. n=5 to 8 biological replicates per group. B, Protein levels of *IRF5* in the heart 28 days after coronary artery ligation and the sham operations were determined by Western blotting. Protein levels were quantified by densitometry and normalized against GAPDH. n=4 to 8 biological replicates per group. Data are presented as mean±standard error of the mean. Values were compared between the MI+PBS and MI+EPA groups using the nonparametric Mann-Whitney U test. *$P<0.05$, **$P<0.01$, comparing the MI+PBS and MI+EPA groups. EPA indicates eicosapentaenoic acid; GAPDH, glyceraldehyde 3-phosphate dehydrogenase; IRF5, interferon regulatory factor 5; MI, myocardial infarction; PBS, phosphate-buffered saline; RTD-PCR, real-time detection polymerase chain reaction.

cardiac rupture are the major causes of death after MI. Cardiac rupture is primarily due to failure in early debridement of necrotic tissue, whereas heart failure is primarily due to impairment of the remodeling process.[3] The incidence of cardiac rupture in the MI+EPA group was comparable to that
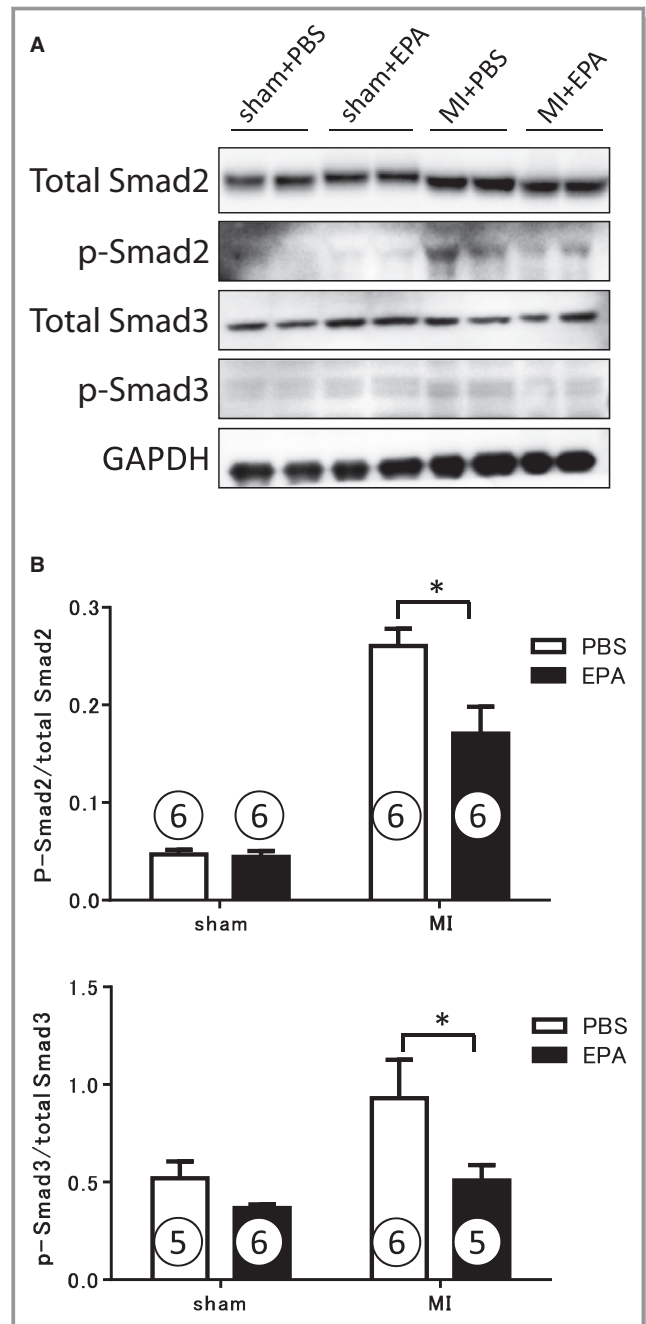

Figure 7. EPA treatment attenuated TGF-β/Smad signaling 28 days after MI. A, Representative Western blots and (B) quantitative analysis of total Smad2, phosphorylated Smad2, total Smad3, phosphorylated Smad3, and GAPDH. Quantitative data were expressed as the ratio between phosphorylated and total protein. n=5 to 6 biological replicates per group. Data are presented as mean±standard error of the mean. Values were compared between the MI+PBS and MI+EPA groups using the nonparametric Mann-Whitney U test. *$P<0.05$, comparing the MI+PBS and MI+EPA groups. EPA indicates eicosapentaenoic acid; GAPDH, glyceraldehyde 3-phosphate dehydrogenase; MI, myocardial infarction; PBS, phosphate-buffered saline; TGF-β, transforming growth factor-β.

in the MI+PBS group. Third, EPA treatment inhibited cardiac dysfunction and dilatation 28 days after MI. Maladaptive post-MI cardiac remodeling was attenuated by EPA treatment during the chronic remodeling phase. Fourth, treatment with EPA attenuated polarization toward proinflammatory M1 macrophages in the infarcted hearts of the mice during the chronic phase. Infiltrating M1 macrophages in the chronically failing heart reestablish a proinflammatory and injurious phenotype[28,39,40] that promotes ongoing remodeling of the noninfarcted area. An example of such remodeling is fibrosis. We therefore concluded that long-term administration of EPA before and after MI improved the prognosis after MI by reducing death from heart failure and attenuated chronic post-MI cardiac remodeling by modulating the activation of proinflammatory M1 macrophages.

The balance between proinflammatory M1 macrophages and reparative M2 macrophages is important in the maintenance and resolution of chronic inflammation in the failing heart. A previous study indicated that siRNA silencing of IRF5, which regulates macrophage polarization toward the proinflammatory M1 phenotype in MI, shifted the macrophage M1 phenotype to the anti-inflammatory M2 phenotype in the heart. In addition, post-MI heart failure was attenuated.[41] Moreover, regulatory T cells were recently recognized to be involved in the macrophage phenotype switch after MI. Genetic or antibody-mediated (anti-CD25) ablation of regulatory T cells leads to M1 macrophage polarization and prolonged inflammation, resulting in adverse cardiac remodeling after MI. Therapeutic regulatory T-cell activation induces M2-macrophage differentiation, which is associated with wound healing after MI.[42] These observations indicated that although appropriate healing required a well-coordinated biphasic macrophage response, a prolonged proinflammatory phase may lead to maladaptive remodeling.[43] In our present study we found that EPA treatment attenuated prolonged activation of proinflammatory M1 macrophages and maladaptive cardiac remodeling during the chronic phase after MI. Moreover, our results indicated that EPA treatment significantly attenuated IRF5, one of the transcription factors that serve as a master regulator of macrophage polarization toward an inflammatory phenotype,[44] in the infarcted heart at both mRNA and protein levels 28 days after MI.

Recent studies indicated that EPA had beneficial effects on macrophage behavior in some disease models. A previous study conducted in the mdx mouse model regarding Duchenne muscular dystrophy indicated that in neuromuscular diseases, EPA decreased inflammation and necrosis in the dystrophic muscle by promoting a shift from the M1 to the M2 macrophage phenotype.[45] In the present study we demonstrated that long-term administration of EPA before and after MI promoted polarization, which is dominated by anti-inflammatory M2 macrophages, and did not affect the total number of macrophages.

In our study, EPA treatment attenuated post-MI cardiac remodeling. However, there is a growing body of evidence to suggest that the beneficial effects of EPA are due to the metabolites rather than the parent compound.[46] For example, one study indicated that dietary enrichment with n-3 fatty acids suppressed choroidal neovascularization, vascular leakage, and immune cell recruitment to the lesion site in a mouse model of laser-induced choroidal neovascularization.[47] In this study, 17,18-epoxyeicosatetraenoic acid derived from EPA and 19,20-epoxydocosapentaenoic acid derived from docosahexaenoic acid, the major cytochrome P450 (CYP)-generated metabolites of these primary n-3 fatty acids, were identified as the key lipid mediators of disease resolution. In cardiovascular diseases treatment with 18-hydroxyeicosapentaenoic acid, a CYP-generated metabolite of EPA,[48] had beneficial effects on pressure overload–induced maladaptive cardiac remodeling by inhibiting macrophage recruitment to the pressure-overloaded heart.[49] In this study the same dose of EPA (administered at a dose of 5 μg by intraperitoneal injection every 3 days from the beginning of pressure overload) had only a small effect on pressure overload–induced cardiac fibrosis and inflammation compared to that of 18-hydroxyeicosapentaenoic acid. However, the dose and duration of EPA administration in this study were much less than those in our study. These results suggested that a higher dose of EPA, as a parent compound, was likely required than that of the metabolites of EPA. Further investigation is needed to determine how much EPA is required to attenuate post-MI cardiac remodeling and how long it should be administered. To more accurately determine the effects of EPA on cardiac remodeling after MI, we need to identify the metabolites derived from EPA, using liquid chromatography–tandem mass spectrometry.

Treatment with EPA attenuated fibrosis in the noninfarcted myocardium and decreased the expression levels of fibrosis-related genes, such as collagen I, collagen III, and TGF-β1, in the infarcted heart 28 days after MI. A 2- to 3-fold increase in myocardial collagen above the normal level resulted in increased LV stiffness and mild dysfunction; however, a very small decrease in collagen below normal levels can result in drastic consequences, including LV dilatation and rupture.[50] In the present study EPA treatment decreased mortality due to heart failure and attenuated postinfarction LV dilatation; however, mortality due to cardiac rupture was similar in the MI+PBS and MI+EPA groups. Some studies reported that EPA attenuated the expression level of TGF-β1,[21,51-53] which played a pivotal role in the development of cardiac fibrosis and hypertrophy. Activation of TGF-β1 is protective against the early phase of ischemic myocardial damage. However, the beneficial effects of TGF-β1 may be lost when its expression is sustained, resulting in LV remodeling and heart failure 28 days after MI.[34] In the present study, although EPA

treatment attenuated TGF-β/Smad signaling via the Smad2 and Smad3 pathway during the chronic remodeling phase, the detailed mechanisms by which EPA treatment attenuates TGF/Smad pathway remain poorly understood. To the best of our knowledge there has been no report that EPA affects posttranscriptional regulation of TGF-β receptors and downstream signaling pathways of TGF-β. In our study the TGF-β production was increased, and TGF-β/Smad signaling was activated during the post-MI chronic remodeling phase; however, these were attenuated by EPA treatment. These results indicated that the inhibition of TGF-β production, but not posttranscriptional regulation of TGF-β receptors and downstream signaling pathways of TGFβ, by EPA treatment played an important role in attenuating post-MI chronic remodeling. One study previously reported that the transcription of TGF-β1 was activated by nuclear factor-κB (NF-κB) and activator protein 1 (AP-1). This activation was triggered by direct recruitment of NF-κB and AP-1 transcription factors to the corresponding binding sites in the TGF-β1 promoter.[54] Another study reported that EPA bound to G-protein-coupled receptor 120 and inhibited NF-κB and JNK.[55] Phosphorylated JNKs activate c-Jun, which is known to form AP-1 transcription factor as a homo- or heterodimer. Taken together, we speculated that the inhibition of TGF-β production played a vital role in regulating TGF-β signaling by EPA treatment during the post-MI chronic remodeling. The results indicated that this was one of the underlying mechanisms through which EPA treatment improved cardiac maladaptive remodeling after MI.

TGF-β1, VEGF, and MRC1 are M2 marker genes. In this study, we observed that EPA administration attenuated the expression level of TGF-β1 only 28 days after MI. In the heart several cell types, including cardiomyocytes, endothelial cells, fibroblasts, and macrophages, release TGF-β1.[38] In addition, EPA prevented the upregulation of the protein and mRNA expression level of TGF-β1 in cultured cardiomyocytes after treatment with endothelin-1.[52] As a result, we believe that in our study, the altered TGF-β1 expression level 28 days after MI was not due to macrophages but, rather, to cardiomyocytes. Nevertheless, further investigation is needed to fully elucidate these speculated events following EPA treatment.

Our study revealed the mechanism underlying the attenuation of post-MI cardiac chronic remodeling after long-term administration of high-dose EPA to mice. However, the results did not reveal a dose- or duration-dependent effect of EPA on post-MI cardiac remodeling. This was because we administered only a high dose of EPA to the mice for a relatively long duration. Furthermore, we did not explore the possibility that the observed effects of EPA were through direct effects of EPA on cardiomyocytes or cell types other than via cardiac M1 macrophage activity. Further studies are therefore required to elucidate the molecular mechanisms (for example, macrophage depletion) underlying the effects of EPA on post-MI cardiac remodeling.

In conclusion, our study indicated that long-term administration of EPA before and after MI improved the prognosis of and attenuated chronic post-MI cardiac remodeling by modulating proinflammatory M1 macrophage activity. Therefore, EPA may be a promising treatment for improving the prognosis of post-MI cardiac remodeling.

Disclosures

None.

References

1. Parikh NI, Gona P, Larson MG, Fox CS, Benjamin EJ, Murabito JM, O'Donnell CJ, Vasan RS, Levy D. Long-term trends in myocardial infarction incidence and case fatality in the National Heart, Lung, and Blood Institute's Framingham Heart study. *Circulation*. 2009;119:1203–1210.

2. Lewis EF, Moye LA, Rouleau JL, Sacks FM, Arnold JM, Warnica JW, Flaker GC, Braunwald E, Pfeffer MA. Predictors of late development of heart failure in stable survivors of myocardial infarction: the CARE study. *J Am Coll Cardiol*. 2003;42:1446–1453.

3. Frangogiannis NG. Regulation of the inflammatory response in cardiac repair. *Circ Res*. 2012;110:159–173.

4. Bang HO, Dyerberg J. Lipid metabolism and ischemic heart disease in Greenland Eskimos. In: Draper H, ed. *Advances in Nutrition Research*. New York, NY: Plenum Press; 1980:1–22.

5. Kagawa Y, Nishizawa M, Suzuki M. Eicosapolyenoic acids of serum lipids of Japanese islanders with low incidence of cardiovascular diseases. *J Nutr Sci Vitaminol (Tokyo)*. 1982;28:441–453.

6. Kromhout D, Bosschieter EB, de Lezenne Coulander C. The inverse relation between fish consumption and 20-year mortality from coronary heart disease. *N Engl J Med*. 1985;312:1205–1209.

7. Kromhout D, Feskens EJ, Bowles CH. The protective effect of a small amount of fish on coronary heart disease mortality in an elderly population. *Int J Epidemiol*. 1995;24:340–345.

8. Albert CM, Hennekens CH, O'Donnell CJ, Ajani UA, Carey VJ, Willett WC, Ruskin JN, Manson JE. Fish consumption and risk of sudden cardiac death. *JAMA*. 1998;279:23–28.

9. Daviglus ML, Stamler J, Orencia AJ, Dyer AR, Liu K, Greenland P, Walsh MK, Morris D, Shekelle RB. Fish consumption and the 30-year risk of fatal myocardial infarction. *N Engl J Med*. 1997;336:1046–1053.

10. Zhao YT, Chen Q, Sun YX, Li XB, Zhang P, Xu Y, Guo JH. Prevention of sudden cardiac death with omega-3 fatty acids in patients with coronary heart disease: a meta-analysis of randomized controlled trials. *Ann Med*. 2009;41:301–310.

11. León H, Shibata MC, Sivakumaran S, Dorgan M, Chatterley T, Tsuyuki RT. Effect of fish oil on arrhythmias and mortality: systematic review. *BMJ*. 2008;337:a2931.

12. Marik PE, Varon J. Omega-3 dietary supplements and the risk of cardiovascular events: a systematic review. *Clin Cardiol*. 2009;32:365–372.

13. Kwak SM, Myung S-K, Lee YJ, Seo HG. Efficacy of omega-3 fatty acid supplements (eicosapentaenoic acid and docosahexaenoic acid) in the secondary prevention of cardiovascular disease: a meta-analysis of randomized, double-blind, placebo-controlled trials. *Arch Intern Med*. 2012;172:686–694.

14. Gruppo Italiano per lo Studio della Sopravvivenza nell'Infarto miocardico. Dietary supplementation with n-3 polyunsaturated fatty acids and vitamin E after myocardial infarction: results of the GISSIPrevenzione trial. *Lancet*. 1999;354:447–455. [Errata, Lancet. 2001;357:642, 2007;369:106.]

15. Macchia A, Levantesi G, Franzosi MG, Geraci E, Maggioni AP, Marfisi R, Nicolosi GL, Schweiger C, Tavazzi L, Tognoni G, Valagussa F, Marchioli R. Left ventricular systolic dysfunction, total mortality, and sudden death in patients with myocardial infarction treated with n-3 polyunsaturated fatty acids. *Eur J Heart Fail*. 2005;7:904–909.

16. Kromhout D, Giltay EJ, Geleijnse JM. n-3 fatty acids and cardiovascular events after myocardial infarction. *N Engl J Med*. 2010;363:2015–2026.

17. Rauch B, Schiele R, Schneider S, Diller F, Victor N, Gohlke H, Gottwik M, Steinbeck G, Del Castillo U, Sack R, Worth H, Katus H, Spitzer W, Sabin G, Senges J. OMEGA, a randomized, placebo-controlled trial to test the effect of highly purified omega-3 fatty acids on top of modern guideline-adjusted therapy after myocardial infarction. *Circulation*. 2010;122:2152–2159.

18. Nilsen DW, Albrektsen G, Landmark K, Moen S, Aarsland T, Woie L. Effects of a high-dose concentrate of n-3 fatty acids or corn oil introduced early after an acute myocardial infarction on serum triacylglycerol and HDL cholesterol. *Am J Clin Nutr*. 2001;74:50–56.

19. Yokoyama M, Origasa H. Effects of eicosapentaenoic acid on cardiovascular events in Japanese patients with hypercholesterolemia: rationale, design, and baseline characteristics of the Japan EPA Lipid Intervention Study (JELIS). *Am Heart J*. 2003;146:613–620.

20. Nakajima K, Yamashita T, Kita T, Takeda M, Sasaki N, Kasahara K, Shinohara M, Rikitake Y, Ishida T, Yokoyama M, Hirata K. Orally administered eicosapentaenoic acid induces rapid regression of atherosclerosis via modulating the phenotype of dendritic cells in LDL receptor-deficient mice. *Arterioscler Thromb Vasc Biol*. 2011;31:1963–1972.

21. Kitamura K, Shibata R, Tsuji Y, Shimano M, Inden Y, Murohara T. Eicosapentaenoic acid prevents atrial fibrillation associated with heart failure in a rabbit model. *Am J Physiol Heart Circ Physiol*. 2011;300:H1814–H1821.

22. He K, Song Y, Daviglus ML, Liu K, Van Horn L, Dyer AR, Greenland P. Accumulated evidence on fish consumption and coronary heart disease mortality: a meta-analysis of cohort studies. *Circulation*. 2004;109:2705–2711.

23. Heydari B, Abdullah S, Pottala JV, Shah R, Abbasi S, Mandry D, Francis SA, Lumish H, Ghoshhajra BB, Hoffmann U, Appelbaum E, Feng JH, Blankstein R, Steigner M, McConnell JP, Harris W, Antman EM, Jerosch-Herold M, Kwong RY. Effect of omega-3 acid ethyl esters on left ventricular remodeling after acute myocardial infarction clinical perspective. *Circulation*. 2016;134:378–391.

24. Ootsuji H, Honda M, Kaneko S, Usui S, Okajima M, Okada H, Sakai Y, Takamura T, Horimoto K, Takamura M. Altered hepatic gene expression profiles associated with myocardial ischemia. *Circ Cardiovasc Genet*. 2010;3:68–77.

25. Usui S, Maejima Y, Pain J, Hong C, Cho J, Park JY, Zablocki D, Tian B, Glass DJ, Sadoshima J. Endogenous muscle atrophy F-box mediates pressure overload–induced cardiac hypertrophy through regulation of nuclear factor-κB. *Circ Res*. 2011;109:161–171.

26. Frantz S, Nahrendorf M. Cardiac macrophages and their role in ischaemic heart disease. *Cardiovasc Res*. 2014;102:240–248.

27. Shinagawa H, Frantz S. Cellular immunity and cardiac remodeling after myocardial infarction: role of neutrophils, monocytes, and macrophages. *Curr Heart Fail Rep*. 2015;12:247–254.

28. Gordon S, Taylor PR. Monocyte and macrophage heterogeneity. *Nat Rev Immunol*. 2005;5:953–964.

29. Han MS, Jung DY, Morel C, Lakhani SA, Kim JK, Flavell RA, Davis RJ. JNK expression by macrophages promotes obesity-induced insulin resistance and inflammation. *Science*. 2013;339:218–222.

30. Fujisaka S, Usui I, Bukhari A, Ikutani M, Oya T, Kanatani Y, Tsuneyama K, Nagai Y, Takatsu K, Urakaze M, Kobayashi M, Tobe K. Regulatory mechanisms for adipose tissue M1 and M2 macrophages in diet-induced obese mice. *Diabetes*. 2009;58:2574–2582.

31. Shiraishi M, Shintani Y, Shintani Y, Ishida H, Saba R, Yamaguchi A, Adachi H, Yashiro K, Suzuki K. Alternatively activated macrophages determine repair of the infarcted adult murine heart. *J Clin Invest*. 2016;126:2151–2166.

32. Yan X, Anzai A, Katsumata Y, Matsuhashi T, Ito K, Endo J, Yamamoto T, Takeshima A, Shinmura K, Shen W, Fukuda K, Sano M. Temporal dynamics of cardiac immune cell accumulation following acute myocardial infarction. *J Mol Cell Cardiol*. 2013;62:24–35.

33. Pinto AR, Paolicelli R, Salimova E, Gospocic J, Slonimsky E, Bilbao-Cortes D, Godwin JW, Rosenthal NA. An abundant tissue macrophage population in the adult murine heart with a distinct alternatively-activated macrophage profile. *PLoS One*. 2012;7:e36814.

34. Ikeuchi M, Tsutsui H, Shiomi T, Matsusaka H, Matsushima S, Wen J, Kubota T, Takeshita A. Inhibition of TGF-β signaling exacerbates early cardiac dysfunction but prevents late remodeling after infarction. *Cardiovasc Res*. 2004;64:526–535.

35. Ismahil MA, Hamid T, Bansal SS, Patel B, Kingery JR, Prabhu SD. Remodeling of the mononuclear phagocyte network underlies chronic inflammation and disease progression in heart failure: critical importance of the cardiosplenic axis. *Circ Res*. 2014;114:266–282.

36. Takaoka A, Yanai H, Kondo S, Duncan G, Negishi H, Mizutani T, Kano S-I, Honda K, Ohba Y, Mak TW, Taniguchi T. Integral role of IRF-5 in the gene induction programme activated by Toll-like receptors. *Nature*. 2005;434:243–249.

37. Krausgruber T, Blazek K, Smallie T, Alzabin S, Lockstone H, Sahgal N, Hussell T, Feldmann M, Udalova IA. IRF5 promotes inflammatory macrophage polarization and TH1-TH17 responses. *Nat Immunol*. 2011;12:231–238.

38. Euler G. Good and bad sides of TGFβ-signaling in myocardial infarction. *Front Physiol*. 2015;6:66.

39. Ingersoll MA, Platt AM, Potteaux S, Randolph GJ. Monocyte trafficking in acute and chronic inflammation. *Trends Immunol*. 2011;32:470–477.

40. Biswas SK, Mantovani A. Macrophage plasticity and interaction with lymphocyte subsets: cancer as a paradigm. *Nat Immunol*. 2010;11:889–896.

41. Courties G, Heidt T, Sebas M, Iwamoto Y, Jeon D, Truelove J, Tricot B, Wojtkiewicz G, Dutta P, Sager HB, Borodovsky A, Novobrantseva T, Klebanov B, Fitzgerald K, Anderson DG, Libby P, Swirski FK, Weissleder R, Nahrendorf M. In vivo silencing of the transcription factor IRF5 reprograms the macrophage phenotype and improves infarct healing. *J Am Coll Cardiol*. 2014;63:1556–1566.

42. Weirather J, Hofmann U, Beyersdorf N, Ramos GC, Vogel B, Frey A, Ertl G, Kerkau T, Frantz S. Foxp3+CD4+ T cells improve healing after myocardial infarction by modulating monocyte/macrophage differentiation. *Circ Res*. 2014;115:55–67.

43. Nahrendorf M, Pittet MJ, Swirski FK. Monocytes: protagonists of infarct inflammation and repair after myocardial infarction. *Circulation*. 2010;121:2437–2445.

44. Lawrence T, Natoli G. Transcriptional regulation of macrophage polarization: enabling diversity with identity. *Nat Rev Immunol*. 2011;11:750–761.

45. de Carvalho SC, Apolinário LM, Matheus SMM, Santo Neto H, Marques MJ. EPA protects against muscle damage in the mdx mouse model of Duchenne muscular dystrophy by promoting a shift from the M1 to M2 macrophage phenotype. *J Neuroimmunol*. 2013;264:41–47.

46. Westphal C, Konkel A, Schunck W-H. Cytochrome p450 enzymes in the bioactivation of polyunsaturated fatty acids and their role in cardiovascular disease. *Adv Exp Med Biol*. 2015;851:151–187.

47. Yanai R, Mulki L, Hasegawa E, Takeuchi K, Sweigard H, Suzuki J, Gaissert P, Vavvas DG, Sonoda K-H, Rothe M, Schunck W-H, Miller JW, Connor KM. Cytochrome P450–generated metabolites derived from ω-3 fatty acids attenuate neovascularization. *Proc Natl Acad Sci USA*. 2014;111:9603–9608.

48. Serhan CN, Chiang N, Van Dyke TE. Resolving inflammation: dual anti-inflammatory and pro-resolution lipid mediators. *Nat Rev Immunol*. 2008;8:349–361.

49. Endo J, Sano M, Isobe Y, Fukuda K, Kang JX, Arai H, Arita M. 18-HEPE, an n-3 fatty acid metabolite released by macrophages, prevents pressure overload-induced maladaptive cardiac remodeling. *J Exp Med*. 2014;211:1673–1687.

50. Jugdutt BI. Ventricular remodeling after infarction and the extracellular collagen matrix: when is enough enough? *Circulation*. 2003;108:1395–1403.

51. Zhang M, Hagiwara S, Matsumoto M, Gu L, Tanimoto M, Nakamura S, Kaneko S, Gohda T, Qian J, Horikoshi S, Tomino Y. Effects of eicosapentaenoic acid on the early stage of type 2 diabetic nephropathy in KKA(y)/Ta mice: involvement of anti-inflammation and antioxidative stress. *Metabolism*. 2006;55:1590–1598.

52. Shimojo N, Jesmin S, Zaedi S, Maeda S, Soma M, Aonuma K, Yamaguchi I, Miyauchi T. Eicosapentaenoic acid prevents endothelin-1-induced cardiomyocyte hypertrophy in vitro through the suppression of TGF-β1 and phosphorylated JNK. *Am J Physiol Heart Circ Physiol*. 2006;291:H835–H845.

53. Kajikawa S, Imada K, Takeuchi T, Shimizu Y, Kawashima A, Harada T, Mizuguchi K. Eicosapentaenoic acid attenuates progression of hepatic fibrosis with inhibition of reactive oxygen species production in rats fed methionine- and choline-deficient diet. *Dig Dis Sci*. 2011;56:1065–1074.

54. Lee K-Y, Ito K, Hayashi R, Jazrawi EPI, Barnes PJ, Adcock IM. NF-κB and activator protein 1 response elements and the role of histone modifications in IL-1β-induced TGF-β1 gene transcription. *J Immunol*. 2005;176:603–615.

55. Oh DY, Talukdar S, Bae EJ, Imamura T, Morinaga H, Fan W, Li P, Lu WJ, Watkins SM, Olefsky JM. GPR120 is an omega-3 fatty acid receptor mediating potent anti-inflammatory and insulin-sensitizing effects. *Cell*. 2010;142:687–698.

SUPPLEMENTAL MATERIAL

Figure S1. EPA attenuated cardiac remodeling and congestive heart failure after MI.
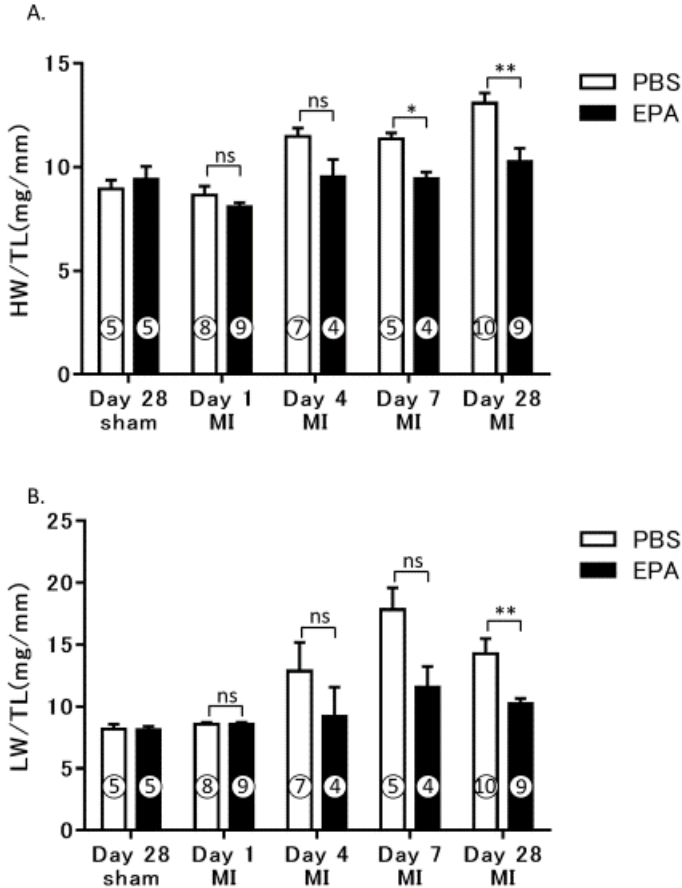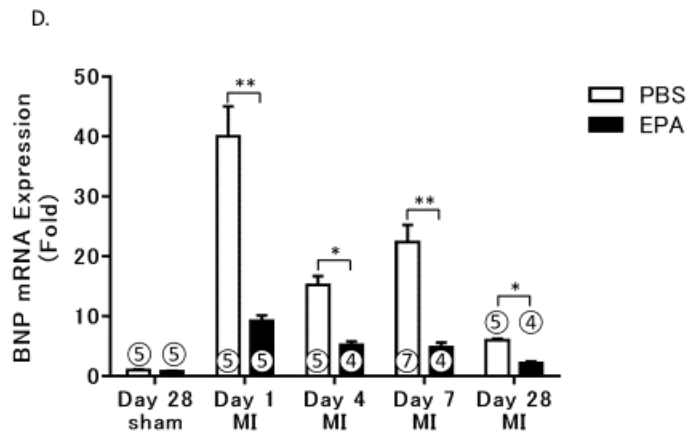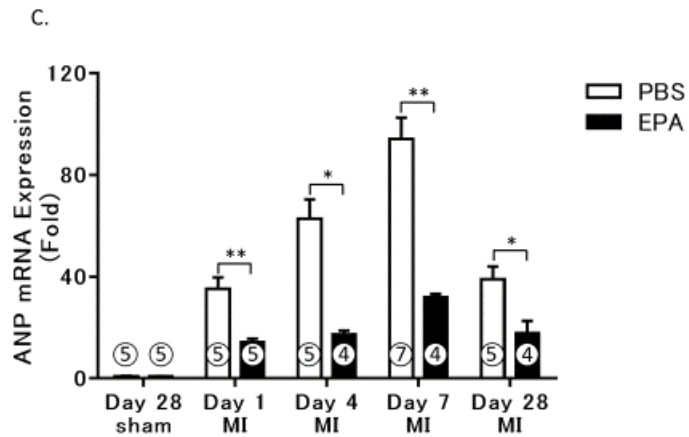
Ratio of (**A**) heart weight to tibial length (HW/TL) and (**B**) lung weight to tibial length (LW/TL),

calculated 1, 4, 7, and 28 days after MI and 28 days after the sham the operation (n = 4 to 10

biological replicates per group). Cardiac mRNA expression levels of (**C**) *ANP* and (**D**) *BNP* 1, 4,

7, and 28 days after coronary artery ligation and 28 days after the sham operation were

determined by RTD-PCR (n = 4 to 7 biological replicates per group). Data are presented as

mean ± standard error of the mean. Values were compared between the MI + PBS and MI +

EPA groups using the nonparametric Mann-Whitney U test. * $P < 0.05$, ** $P < 0.01$, comparing

the MI + PBS and MI + EPA groups. EPA, eicosapentaenoic acid; MI, myocardial infarction;

PBS, phosphate-buffered saline.

Figure S2. Echocardiographic analyses of the sham + PBS (n = 3), sham + EPA (n = 3), MI +

PBS (n = 7), and MI + EPA (n = 5) groups 1, 4, 7, and 28 days after the sham and MI

operations.
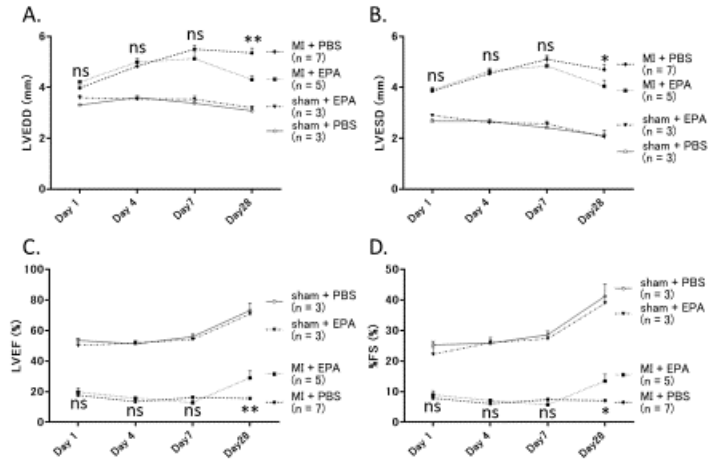
(**A**) LVEDD, (**B**) LVESD, (**C**) EF and (**D**) %FS. Data are presented as mean ± standard error of
the mean. Values were compared between the MI + PBS and MI + EPA groups using the
nonparametric Mann-Whitney U test. * P < 0.05, ** P < 0.01, comparing the MI + PBS and MI +
EPA groups. EPA, eicosapentaenoic acid; LVEDD, left ventricular end-diastolic diameter; LVEF,
left ventricular ejection fraction; LVESD, left ventricular end-systolic diameter; MI, myocardial
infarction; PBS, phosphate-buffered saline; %FS, percentage fractional shortening.